

Buoyancy effect on atmospheric surface layer: measurements from the East Coast of Malaysia

Z. Harun^{1,2}, E. Reda¹ and Rozli Zulkifli¹

¹Dept. Mechanical and Materials, Faculty of Engineering and Built Environment, Universiti Kebangsaan Malaysia, UKM Bangi, 43600, Malaysia

²Marine Ecosystem Research Centre (EKOMAR), Faculty of Science and Technology, Universiti Kebangsaan Malaysia, UKM Bangi, 43600, Malaysia

E-mail: zambri@ukm.edu.my

Abstract. The nature and evolution of the atmospheric surface layer is still unresolved completely. Many questions regarding the existence of the z-less layer and trend of the cross correlations still remain open. This research analyzes some of the surface layer ambiguities. In this research temperature, velocity and turbulence data were collected from a weather station facility located in the Marine Ecosystem Research Centre (EKOMAR) Mersing on the East Coast of Malaysia. Two high resolution hotwires were utilized at 3 m and 12 m heights above ground. Both gradient Richardson number and Obukhov stability parameter were calculated. Turbulence spectra were plotted at different stability conditions. The results does not show the existence of the z-less layer at deep stable condition. The buoyancy force, under unstable condition, was found responsible for the increase of vertical correlation factor. The fingerprint of the buoyancy force was detected in the spectra at low frequencies.

1. Introduction

The complete understanding of turbulence structure of the atmospheric boundary layer (ABL) is indispensable for the assessment of air pollutant dispersion, natural ventilation through cities and urban heat island intensity. In addition, computational fluid dynamics (CFD) simulations of atmospheric flows rely on experimental data to develop turbulence models and provide realistic boundary conditions and wall functions [1–5]. Much research has been conducted in atmospheric turbulence through the last seven decades since the pioneering work of Monin and Obukhov. Under strong stability conditions all turbulence statistics are expected to be independent of the height z above ground [6, 10]. However, [7] argued that z-less concept holds only for non-dimensional standard deviation of temperature.

The two-point correlation of turbulence in ABL was held by [8] to quantify the structure inclination angle of coherent flow structures. The more unstable the surface layer, the higher the inclination angle in the windward direction with a value of 12° at neutrally stable condition, despite earlier study by [17] who found structure inclination angle to be invariant over three order of the Reynolds number. The two-point vertical correlation was adopted by [9] who found the streamwise and vertical wind components to show little dependence on the turbulence intensity. The spectral analysis of wind components at unstable condition reveals the existence of a spectral region of 2 slope at lower frequencies, indicating the presence of a buoyancy subrange supporting two-dimensional motions [11]. Although the widespread use of ultrasonic anemometers in atmospheric flow measurements, the hot wire anemometry is still a preferred



technique for fundamental turbulence studies thanks to its high temporal and spacial resolution [12, 16].

This work aims at enriching the atmospheric turbulence database by reproducing some of the basic correlations using hot wire anemometer measurements at different heights. In this research thermal, mean and turbulent data were collected from Mersing at the East Coast of Malaysia over eleven days (25 March - 5 April, 2016) in the period between the flooding and dry monsoons in Malaysia. A full description of the site and the experimental setup is given in Section 2. The results are illustrated and discussed in Section 3. Finally, the conclusions are listed in Section 4.

2. Method

2.1. Site description

The EKOMAR site ($2^{\circ}34'42.11''\text{N}$, $103^{\circ}48'21.05''\text{E}$) lies on the East Coast of Malaysia, approximately 22 km to the north of Mersing. The pictures in Figure 1 show the entire field facility; it consists of 60 m pole and newly installed 12 m pole for this research. Instrumentation were installed 150 m away from sea line (at high tide) with only a 1 m height site fence and one medium size tree (100 m ahead) in-between. Ground topography is plain and its level is 0.5 m above sea level; the level changes abruptly 100 m away from the instrumentation. Land is covered with 5 cm grass until the sharp level change.



(a) The weather station infrastructure, EKOMAR (b) EKOMAR snapshot taken approximately from the South, showing the South China Sea. snapshot taken from the West, showing the 12 m pole. The 60 m pole to the right was also utilized, but not discussed here. An intermediary pole in between the two (not clear) was used for the 3 m position.

Figure 1. The EKOMAR weather station, Tangjung Langsat, Endau Johor.

2.2. Instrumentation

Two hotwire probes (5 micron wire diameter) were installed on two adjacent columns (2 m apart) of heights 3 and 12 m. The wires were set vertical such that they read the horizontal magnitude of the wind speed. Samples were acquired at 12 Hz. Each probe was replaced with another calibrated one daily. Calibrations were held in-situ by the Dantec[®] calibrator. The adverse weather made hotwire measurement more difficult. The authors had to install the entire hotwire etching facility in the EKOMAR laboratory. With this facility, etching the wollaston wire to expose approximately 1.5 mm platinum was possible. A weather station was used to measure temperature, wind speed and direction. It was placed in the middle distance between

the two columns at 1.7 m above ground level. The station could captured data continuously. Another temperature sensor was fixed on the 12 m pole. The details of employed devices are listed in Table 1. Data were arranged in continuous sampling groups each of which is 30 minutes long (sampling time) to form a total of 327 groups (163.5 hours of continuous and discrete data).

Table 1. Specs of the utilized instruments.

Sensor	Type and model	Specifications
Hotwire anemometry	5 micron wires Dantec [®] 54N80 Multichannel Anemometer	Range*: 0.4~46.5 m/s Accuracy*: ± 0.2 m/s at 11 m/s
Weather station	Rainwise [®] MK-III	Wind speed Range: 0~67 m/s Accuracy: Greater of 0.45 m/s or 5% of Reading Wind direction Range: 0~360° Accuracy: $\pm 11.25^\circ$ Temperature Range: -55~85° C Accuracy: $\pm 0.2^\circ$ C at 25° C
Temperature sensor	Comet [®] H6320	Range: -30~60° C Accuracy: $\pm 0.4^\circ$ C

* Based on in-situ calibration data.

2.3. Parameters

2.3.1. Stability parameters Two stability parameters were considered in this study; the Obukhov stability parameter (ζ) and gradient Richardson number (Ri_g) both defined here as following:

$$\zeta = \frac{z}{L} = \frac{z\kappa g\theta^*}{u_*^2\Theta} \quad (1)$$

$$Ri_g = \frac{\frac{g}{\Theta} \frac{\partial \Theta}{\partial z}}{\frac{\partial U^2}{\partial z}} \quad (2)$$

where L is the Obukhov length, z is the height above ground level, κ is Von Karman constant taken here as 0.41, g is the gravitational acceleration (9.81 m/s^2), U and Θ are the time mean wind speed and potential temperature and u_* and θ_* are the friction velocity and friction temperature. In this research, both the friction velocity and temperature were calculated using the Monin-Obukhov similarity theory as follows:

$$u_* = \frac{\kappa \Delta U}{\ln \left(\frac{z_2}{z_1} \right) - (\psi_{M2} - \psi_{M1})} \quad (3)$$

$$\theta_* = \frac{\kappa \Delta \Theta}{\ln \left(\frac{z_2}{z_1} \right) - (\psi_{H2} - \psi_{H1})} \quad (4)$$

The two of ψ_M and ψ_H are functions of the stability parameter ζ . The Businger-Dyer relations [13] were adopted to calculate ψ_M and ψ_H as below:

For **stable** surface layer ($\zeta > 0$):

$$\psi_M = \psi_H = -5\zeta \quad (5)$$

For **unstable** surface layer ($\zeta < 0$):

$$\psi_M = 2\ln\left(\frac{1+X}{2}\right) + \ln\left(\frac{1+X^2}{2}\right) - 2\tan^{-1}X + \frac{\pi}{2} \quad (6)$$

$$\psi_H = 2\ln\left(\frac{1+X^2}{2}\right) \quad (7)$$

$$X = (1 - 16\zeta)^{\frac{1}{4}} \quad (8)$$

2.4. Analysis

To calculate the potential temperature, the pressure at the ground level (measured by the weather station) was set as a reference pressure while the barometric pressure at 12 m height was calculated from ideal gas laws. The mean velocities at 1.7 and 12 m were used to calculate Ri_g , u^* and θ^* . A power spectral density (PSD) analysis was held for the data measured by both hotwires and a Kaiser window [14] was applied to the time series data to remove the undesired noise.

3. Results and discussion

3.1. The weather description

A three-day sample of the temperature and wind speed and direction data gathered by the weather station is shown in Figure 2(a) and Figure 2(b), respectively. The temperature pattern in the sample does not reflect typical Malaysian weather [18] because the field trip was made during a period where El Nino phenomenon was believed to have occurred. The wind speeds have been very steady for the three-day sample at 3 m/s - 5 m/s. The wind direction is very stable where 30 degrees is actually reflecting winds coming from the open seas.

3.2. Turbulence intensities

Figure 3 illustrates the normalized turbulence intensity as a function of Obukhov stability parameter. It is obvious that the intensity fits an asymptotic constant-value line as the surface layer approaches the neutral condition, Figures 3(a) and 3(b). However, at strong stable/unstable conditions ($|\zeta| \gtrsim 0.1$) the turbulence intensities show sharp increase rather than settling at a constant value which does not agree with the existence of the z-less zone. The fitting line tends to a value of 2.1917 from the unstable side and to 2.5772 from the stable side, which is quite around the well-known value of 2.3.

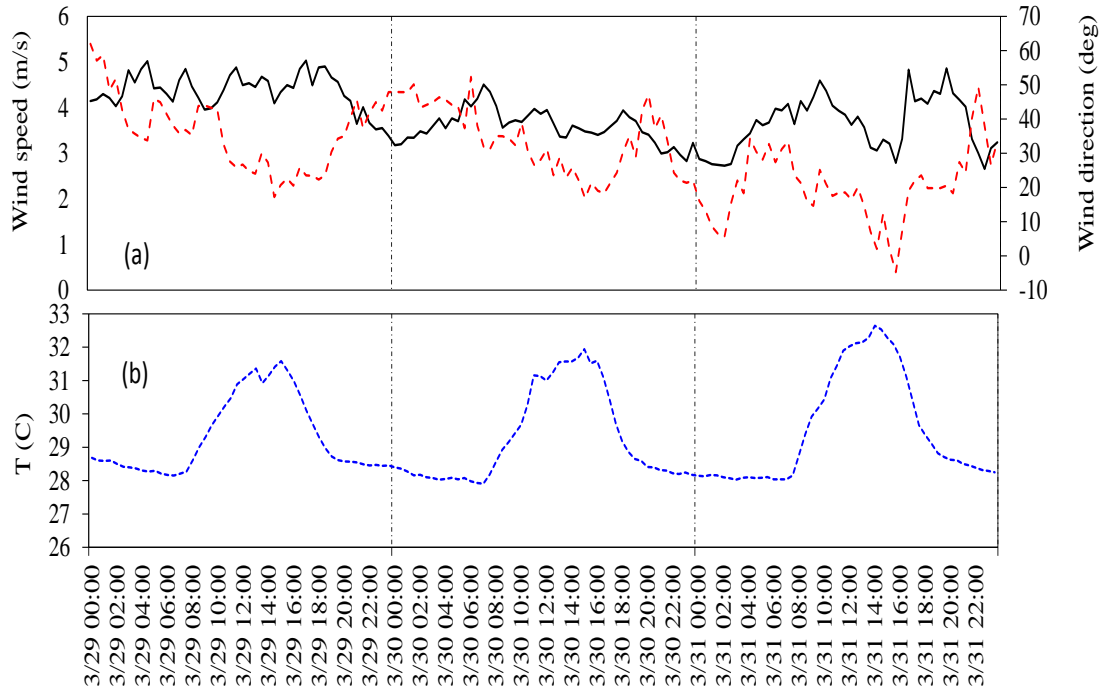


Figure 2. Time series data from the weather station ($z = 1.7$ m) for the period 29-31 March 2016: (a) wind speed (solid line) and direction (dashed red line) (b) temperature.

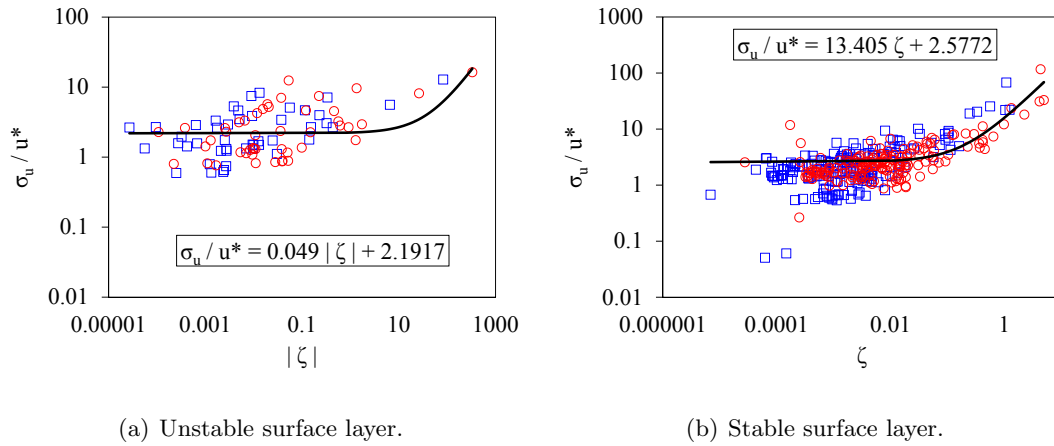


Figure 3. Turbulence intensity as a function of ζ for unstable surface layer (a) and stable surface layer (b). Profiles of normalized turbulence intensity at $z = 3$ m (\square), at $z = 12$ m (\circ) and total data fitting line (solid line).

3.3. Vertical correlations

The variation of the correlation between the two hotwires' velocity components and the gradient Richardson number at the two conditions are illustrated in Figure 4. In unstable condition (Figure 4(a)) the correlation between the two heights increases as the Richardson number decreases (thermal stratification strengthens) [8, 15]. This emphasizes the prominent effects of buoyancy force in mixing the surface layer and breaking down the inclined turbulent flow structures. On the other hand the correlation factor shows almost no dependency on the Ri_g

for stable flow (Figure 4(b)).

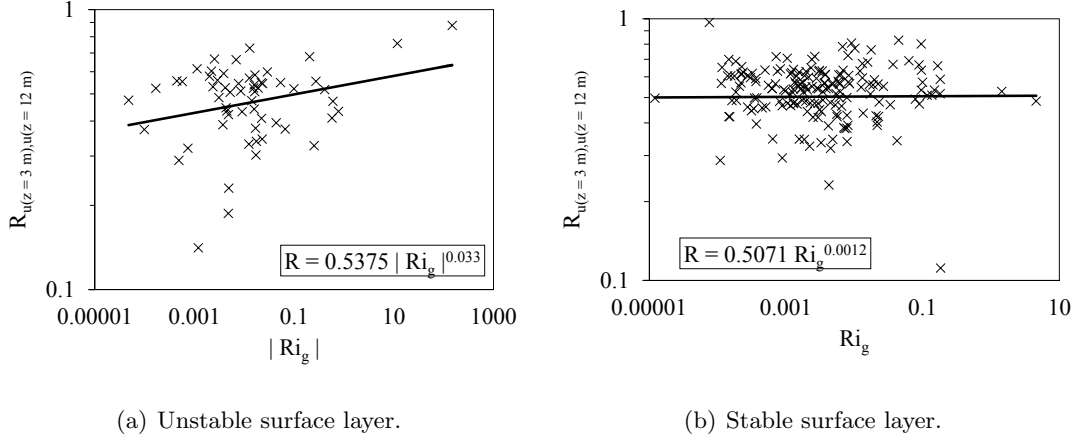


Figure 4. Cross correlation factor between the velocities measures by the two hotwires as a function of Ri_g for unstable surface layer (a) and stable surface layer (b). Profiles of correlation factor (x) and fitting line (solid line).

3.4. Turbulence spectral analysis

Figure 5 shows the spectral analysis of the two hotwires' measurements at unstable ($Ri_g = -148.3$), neutrally stable ($Ri_g \approx 0$) and stable conditions ($Ri_g = 77.82$) where n is the frequency and S_u is the power spectral density function. For both heights, the spectrum of the unstable surface layer experiences a peak at low frequencies, being influenced by buoyant vortical structures. The peak degrades gradually until completely restoring the classic turbulent spectrum profile at profound stable surface layer.

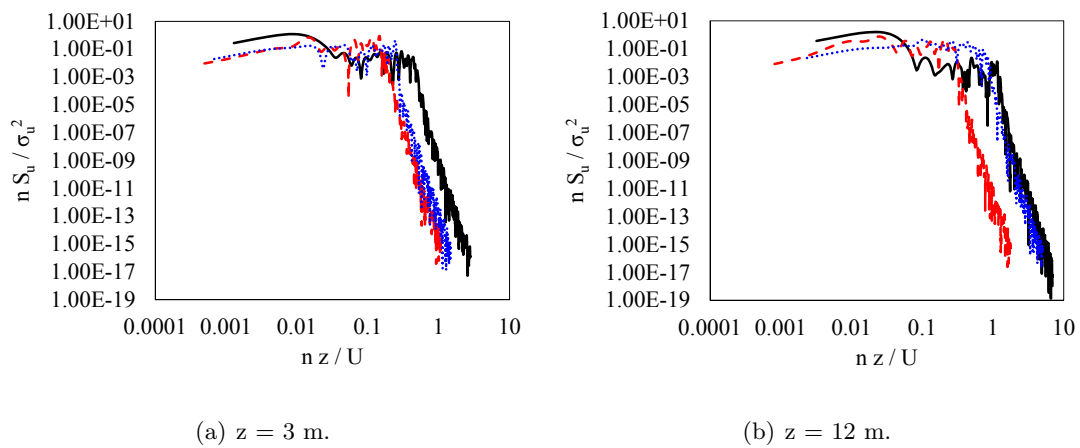


Figure 5. Spectral analysis of velocity components measured by the 3 m level hotwire (a) and the 12 m level hotwire (b). Profiles at unstable condition ($Ri_g = -148.3$) (solid line), neutral stability condition ($Ri_g \approx 0$) (dashed line) and stable condition ($Ri_g = 77.82$). (dotted line).

4. Conclusions

This research sheds light on some of atmospheric layer open questions. 163.5 hours of temperature, velocity and high precision turbulence data were collected from Mersing on the East Coast of Malaysia. The data denies the existence of the z-less zone in very stable surface layer. Also the data showed the effect of buoyancy force in mixing the flow which raises the vertical correlation factor. The buoyant vortical structure was found to alter the turbulence power spectra at low frequencies.

5. Acknowledgement

The author would like to thank the Ministry of Education for providing the Exploratory Research grant. The author would like to express their gratitude for the facility provided at EKOMAR under the Faculty of Science and Technology, UKM.

References

- [1] Hargreaves DM Wright N G 2007 *Journal of Wind Engineering and Industrial Aerodynamics* **95** 355–369
- [2] Lignarolo L, Gorié C, Parente A and Benocci C 2011 Large eddy simulation of the atmospheric boundary layer using openFOAM *13th International Conference on Wind Engineering–Amsterdam, The Netherlands*
- [3] Defraeye T, Blocken B and Carmeliet J 2011 *Building and Environment* **46** 2130–2141
- [4] OSullivan J, Archer R and Flay R 2011 *Journal of Wind Engineering and Industrial Aerodynamics* **99** 65–77
- [5] Xie Z T and Castro I P 2009 *Atmospheric Environment* **43** 2174–2185
- [6] Wyngaard J and Coté O 1972 *Quarterly Journal of the Royal Meteorological Society* **98** 590–603
- [7] Pahlow M, Parlange M B and Porté-Agel F 2001 *Boundary-Layer Meteorology* **99** 225–248
- [8] Chauhan K, Hutchins N, Monty J and Marusic I 2013 *Boundary-Layer Meteorology* **147** 41–50
- [9] Teichrieb C A, Acevedo O C, Degrazia G A, Moraes O L, Roberti D R, Zimmermann H R, Santos D M and Alves R C 2013 *Physica A: Statistical Mechanics and its Applications* **392** 1510–1521
- [10] Nieuwstadt F T 1984 *Journal of the Atmospheric Sciences* **41** 2202–2216
- [11] Cuxart J, Yagüe C, Morales G, Terradellas E, Orbe J, Calvo J, Fernández A, Soler M, Infante C, Buenestado P *et al.* 2000 *Boundary-Layer Meteorology* **96** 337–370
- [12] Lomas C G 2011 *Fundamentals of hot wire anemometry* (Cambridge University Press)
- [13] Dyer A 1974 *Boundary-Layer Meteorology* **7** 363–372
- [14] Kuo F F and Kaiser J F 1966 *System analysis by digital computer* (Wiley)
- [15] Himmema S E and Adrian R J 2003 *Boundary-Layer Meteorology* **106** 147–170
- [16] Hutchins N, Nickels T B, Marusic I and Chong M S 2009 *J. Fluid Mech.* **635** 103–136
- [17] Marusic I and Heuer W D C 2007 *Phys. Review Letter* **99** 41–45
- [18] Latif M T, Dominick D, Ahamad F, Khan M F, Juneng L, Hamzah F M and Nadzir M S M 2014 *Sc. of the Total Environment* **482-483** 336–348